JOURNAL OF VIROLOGY, Apr. 2010, p. 3949–3961 Vol. 84, No. 8
0022-538X/10/$12.00 doi:10.1128/JVI.02085-09

Pathogenesis of a Model Gammaherpesvirus in a Natural Host[▽]

David J. Hughes,[1,3]† Anja Kipar,[2] Jeffery T. Sample,[3]† and James P. Stewart[1]*

School of Infection and Host Defence[1] and Department of Veterinary Pathology,[2] University of Liverpool, Liverpool, United Kingdom, and Department of Biochemistry, St. Jude Children's Research Hospital, Memphis, Tennessee 38105[3]

Received 2 October 2009/Accepted 25 January 2010

Murine gammaherpesvirus 68 (MHV-68) infection of laboratory mice (*Mus musculus*) is an established model of gammaherpesvirus pathogenesis. The fact that *M. musculus* is not a host in the wild prompted us to reassess MHV-68 infection in wood mice (*Apodemus sylvaticus*), a natural host. Here, we report significant differences in MHV-68 infection in the two species: (i) following intranasal inoculation, MHV-68 replicated in the lungs of wood mice to levels approximately 3 log units lower than in BALB/c mice; (ii) in BALB/c mice, virus replication in alveolar epithelial cells was accompanied by a diffuse, T-cell-dominated interstitial pneumonitis, whereas in wood mice it was restricted to focal granulomatous infiltrations; (iii) within wood mice, latently infected lymphocytes were abundant in inducible bronchus-associated lymphoid tissue that was not apparent in BALB/c mice; (iv) splenic latency was established in both species, but well-delineated secondary follicles with germinal centers were present in wood mice, while only poorly delineated follicles were seen in BALB/c mice; and, perhaps as a consequence, (v) production of neutralizing antibody was significantly higher in wood mice. These differences highlight the value of this animal model in the study of MHV-68 pathogenesis.

Human gammaherpesviruses are clinically important lymphotropic pathogens represented by Epstein-Barr virus (EBV) and Kaposi's sarcoma-associated herpesvirus (KSHV) (alternatively, human herpesvirus 8 [HHV-8]). Due to their narrow host range, developing animal model systems of infection is problematic, and consequently, it is difficult to accurately investigate pathogeneses associated with these viruses. While attempts have been made to investigate the pathogeneses of EBV and KSHV by infecting nonhuman primates, these hosts do not accurately recapitulate human disease, and in some cases, infection results in a lack of detectable virus-specific antibodies or viral-gene transcription (31). Alternatively, simian homologues of these human viruses do exist (rhesus lymphocryptovirus [RhLCV], similar to EBV; retroperitoneal fibromatosis herpesvirus [RFHV] and rhesus rhadinovirus [RRV], similar to KSHV), and it has been established that infection of rhesus macaques with these viruses mimics human disease more effectively (9, 29, 32). However, for numerous reasons, primate studies are not always feasible. Nonetheless, such studies have highlighted the importance of infection in the context of a natural host for accurate modeling of infection and pathogenesis associated with the gammaherpesviruses.

Murine gammaherpesvirus isolate 68 (MHV-68)—officially murid herpesvirus type 4 (MuHV-4) and also commonly gammaherpesvirus 68—naturally infects murid rodents (3, 13), offering a potential alternative model of human gammaherpesvirus infection through experimental infection of inbred laboratory strains of mice with MHV-68. Indeed, this model has advanced or complemented what is known about the pathogenesis of the human gammaherpesviruses. Characteristically, infection of laboratory mice with MHV-68 via the intranasal route involves productive virus replication in the lung that, in spite of a specific cytotoxic T-lymphocyte (CTL) response to infected cells, yields high titers of infectious virus (40). Concomitant with this lytic infection, the virus establishes latent infection within epithelial and B cells in the lungs (18, 38). From the lungs, the virus spreads to the spleen via the mediastinal lymph nodes (MLN), where latency is predominately established within splenic B cells, though macrophages and dendritic cells also harbor latent infections (17, 19, 22, 28, 46, 48). The establishment of latency in laboratory mice is associated with a sharp increase in the number of splenic leukocytes (leukocytosis) and a large increase in spleen size (splenomegaly), which peak around day 14 postinfection (p.i.) (42). Leukocytosis, which involves the proliferation of both B and T lymphocytes, is dependent on MHV-68-infected B cells and is $CD4^+$ T-cell driven (15, 40, 42).

MHV-68 infection in common laboratory strains of mice (e.g., BALB/c, 129, and C57BL/6) has been intensely studied for more than a decade. We have shown by sequencing, as well as serology, that, in the wild, MHV-68 is a natural pathogen of wood mice (*Apodemus sylvaticus*) (3, 14). However, it is not found in *Mus musculus* (including house mice) (1, 14). Indeed, free-living *M. musculus* mice carry their own distinct gammaherpesvirus (14). Thus, what is known regarding the pathogenesis of MHV-68, although invaluable, has come from the infection of laboratory mice that are not an authentic host. We reasoned, therefore, that the normal pathogenesis of MHV-68 infection may be significantly different than that observed in laboratory mice and that an analysis of MHV-68 infection of a natural host may provide important new insights into gammaherpesvirus biology. Here, we addressed this by comparing the infection of MHV-68-negative, laboratory-bred wood mice to that of BALB/c mice, a commonly used laboratory model host. Although we used only one strain of laboratory mice to study MHV-68 pathogenesis, the study of other inbred strains (e.g.,

* Corresponding author. Mailing address: School of Infection and Host Defence, The University of Liverpool, Duncan Building, Daulby Street, Liverpool L69 3GA, United Kingdom. Phone: 44-151-706-4381. Fax: 44-151-706-5805. E-mail: j.p.stewart@liverpool.ac.uk.

† Present address: Department of Microbiology and Immunology, Pennsylvania State University College of Medicine, Hershey, PA 17033.

▽ Published ahead of print on 3 February 2010.

129 and C57BL/6) has shown only minor differences in pathogenesis and host response, with none being more resistant or susceptible, as seen with other viruses (8, 39). We report important differences that shed new light on MHV-68 pathogenesis: (i) significantly lower virus replication in the lungs of wood mice, much of which occurs in focal, macrophage-rich (granulomatous) inflammatory infiltrates; (ii) augmented viral latency in wood mouse lungs in B cells within inducible bronchus-associated lymphoid tissue (iBALT) that forms during acute infection; (iii) virus latency in well-defined splenic germinal centers as opposed to within poorly organized follicles in BALB/c mice; (iv) efficient establishment of long-term latency in the spleen with less intense leukocytosis and splenomegaly than is seen during acute infection within laboratory strains of *M. musculus*; and (v) significantly greater production of MHV-68 neutralizing antibody in wood mice, perhaps as a consequence of a more highly ordered germinal-center reaction.

MATERIALS AND METHODS

Cell culture and virus stocks. Baby hamster kidney (BHK-21) cells were maintained in Glasgow's modified minimal essential medium supplemented with 10% newborn calf serum and 10% tryptose-phosphate broth, 2 mM L-glutamine, 70 μg/ml penicillin, 10 μg/ml streptomycin. NIH 3T3 cells were maintained in Dulbecco's modified Eagle's medium (DMEM) supplemented with 10% fetal calf serum, 2 mM L-glutamine, 70 μg/ml penicillin, and 10 μg/ml streptomycin. Murid herpesvirus 4 (MHV-68) was originally isolated during field studies from the bank vole, *Myodes glareolus* (4), and was subsequently plaque purified on BHK-21 cells to obtain clone g2.4 (used here), as described previously (12). Viruses were propagated and titrated using BHK-21 cells, as described previously (40).

Wood mouse colony. Wood mice (*Apodemus sylvaticus*) were obtained from an outbred colony established at the University of Liverpool, Faculty of Veterinary Science (2, 16). This colony was obtained from J. Clarke in 1995 and derived from captive-bred colonies maintained for several decades in the Department of Zoology, University of Oxford, with only occasional introductions of new stock from the wild. Their general housing and maintenance have been described elsewhere (10), and at Liverpool, they are maintained under semibarrier conditions. The Liverpool colony has suffered no clinical disease. Although not specified pathogen free (SPF) in the sense used for most laboratory rodents, the animals are tested every month for the major infections of laboratory rodents and for pathological lesions (Harlan United Kingdom Technical Services, Loughborough, United Kingdom) and have so far been negative. Of particular relevance to this study, no evidence of MHV-68 infection has been found in the colony by serology and PCR analysis (3).

Infection of animals. All animal work was performed under United Kingdom Home Office Project License number 40/2483 and Personal License number 60/6501. BALB/c mice were purchased from Bantin and Kingman (Hull, United Kingdom). All animals were female and 5 to 8 weeks of age. The animals were anesthetized with isoflurane and inoculated with 4×10^5 PFU in 40 μl of sterile phosphate-buffered saline (PBS). At various times between days 3 and 40 p.i., animals were euthanized and tissues were harvested.

Virological analysis. Plaque assays to determine infectious virus titers in tissues were performed on homogenized lung tissue using NIH 3T3 cells as previously described (40). Splenocytes purified from intact spleens were examined for levels of latent virus using an infective-center assay, as described previously (40).

Real-time quantitative PCR (qPCR) analysis. To determine the viral-DNA load, DNA was extracted from splenic and pulmonary tissue using DNeasy kits (Qiagen) and quantified by UV spectrophotometry. Quantification of viral DNA copy numbers was performed using an Opticon Monitor 2 real-time PCR machine (MJ Research). Amplification was performed in 20-μl reaction volumes with 200 ng of input DNA using a DyNamo SYBR green kit (Finnzymes). The cycling parameters were as follows: hot start at 95°C for 10 min, denaturation at 94°C for 10 s, annealing at 60°C for 20 s, and extension at 72°C for 15 s. Melting-curve analysis was carried out between 65 and 95°C with 0.2° increments to confirm the specificity of the amplification. A 159-bp portion of the MHV-68 *gp150* gene was amplified using forward primer 5′-CTACTTCTTCATCGGAC GCT-3′ and reverse primer 5′-CGGGATCTGTCGGACTGT-3′ (MWG Biotech). The viral genome copy number was estimated against a standard curve constructed by serially diluting a plasmid containing the 159-bp *gp150* fragment (pCR2.1/gp150; Invitrogen). The murine ribosomal protein L8 gene (*rpl8*; accession no. AF091511) was used to normalize for input DNA between samples. The standard curve for *rpl8* was constructed by serial dilution of a plasmid containing a 163-bp fragment of *rpl8* (pCR2.1/rpl8; Invitrogen). Amplifications of *rpl8* and pCR2.1/rpl8 were carried out using forward primer 5′-CAGTGAATATCGGC AATGTTTTG-3′ and reverse primer 5′-TTCACTCGAGTCTTCTTGGTCT C-3′ (MWG Biotech). Mean viral genome copy numbers were determined from three or four individual animals.

Histology, immunohistology, and RNA *in situ* hybridization. Sections from lungs, mediastinal lymph nodes, and spleen from all animals were fixed in 4% buffered paraformaldehyde, pH 7.4, and routinely embedded in paraffin wax. Sections (3 to 5 μm) were cut and stained with hematoxylin and eosin or used for immunohistology and RNA *in situ* hybridization (RNA-ISH).

Immunohistology was performed to detect viral antigen, to identify infiltrating leukocytes and follicular dendritic cells (FDCs), and to highlight cellular turnover, using both the peroxidase anti-peroxidase (PAP) method and the avidin biotin peroxidase complex (ABC) method, as described previously (23). For the detection of MHV-68 antigen, a polyclonal rabbit antiserum was used that had been generated in rabbits injected with purified MHV-68 particles. T cells were detected by a cross-reacting rabbit anti-human CD3 antibody (DakoCytomation), and B cells were identified using rat anti-mouse CD45R (clone RA3-6B2; SouthernBiotech) in BALB/c and wood mice. Macrophages were identified using rat anti-mouse F4/80 antigen (clone Cl:A3-1; Serotec) and a cross-reacting rabbit antibody against human lysozyme (DakoCytomation) that also stains FDCs. Mouse anti-proliferating cell nuclear antigen (PCNA) (clone PC10; DakoCytomation) identified proliferating cells. In BALB/c mice, germinal-center B cells were identified by binding to biotinylated peanut agglutinin (PNA) (Sigma) (40a). PNA staining failed in wood mice.

RNA-ISH followed previously published protocols (24) and used digoxigenin (DIG) (Roche)-labeled sense and antisense transcripts of MHV-68 tRNA-like molecules 1 to 4, which were generated from plasmid pEH1.4, as described previously (5). Briefly, sections were treated with proteinase K (0.26 μg/ml; Roche) at 37°C for 15 min. Hybridization was performed for 15 to 18 h at 37°C. Stringent posthybridization washes were carried out at 50°C, and hybridized probe was detected with alkaline phosphatase-conjugated anti-DIG Fab fragments (Roche) with 5-bromo-4-chloro-3-indolyl phosphate–nitroblue tetrazolium (BCIP-NBT) substrate (Sigma). Slides were counterstained for 10 s with Papanicolaou's hematoxylin (1:20 in distilled water; Merck Eurolab GmbH, Darmstadt, Germany).

Enzyme-linked immunosorbent assay (ELISA) detection of MHV-68-specific antibody. Virus was extracted from MHV-68-infected BHK-21 cells by Dounce homogenization and diluted in PBS, inactivated under UV light, and used to coat Immulon 4HBX plates (Thermo Life Sciences) for 24 h at 4°C. The plates were then washed five times with PBS-Tween (0.01%) and blocked with PBS-Tween with 2% normal rabbit serum (DakoCytomation) for 1 h at 37°C. Twofold dilutions of sera, starting with an initial dilution of 1:20 in PBS-Tween with 2% normal rabbit serum, were added to the wells of the plates and incubated at 37°C for 1 h, followed by an additional five washes. Rabbit anti-mouse immunoglobulin conjugated to horseradish peroxidase (HRP) (Dako) diluted 1:1,000 was added to the plates and incubated for 1 h at 37°C, followed by five washes. Finally, bound antibody was detected by adding *o*-phenylenediamine dihydrochloride (OPD) (Sigma) as a peroxidase substrate, incubation at room temperature for 30 min in the dark, and measurement of absorbancy at 450 nm. Antibody levels were expressed as the reciprocal dilution at which the sample became negative (determined as the mean absorbance value of normal mouse sera plus 2 standard deviations). Mean absorption values were taken from three or four individually infected animals.

Virus neutralization assay. Virus neutralization assays were carried out as previously described (37). Sera were incubated at 56°C for 30 min to inactivate complement. Twofold dilutions of sera ranging from 1:10 to 1:160 were mixed with 200 PFU MHV-68 and incubated for 1 h at 37°C. The virus-serum mixture was then added to subconfluent NIH 3T3 cells and incubated for 1 h at 37°C to allow adsorption of nonneutralized virus. The cells were then washed 3 times, overlaid with fresh medium containing 3.5 g/liter carboxymethylcellulose, and incubated for 4 days at 37°C, after which the cell monolayer was fixed and stained. The data were presented as the mean reciprocal dilution (of 3 individual serum samples per time point, plus or minus the standard deviation) required to cause a 50% reduction in the number of plaques.

Statistical analyses. Two-way analysis of variance (ANOVA) tests with Bonferroni posttests or *t* tests were performed; *P* values were set at a 95% confidence interval.

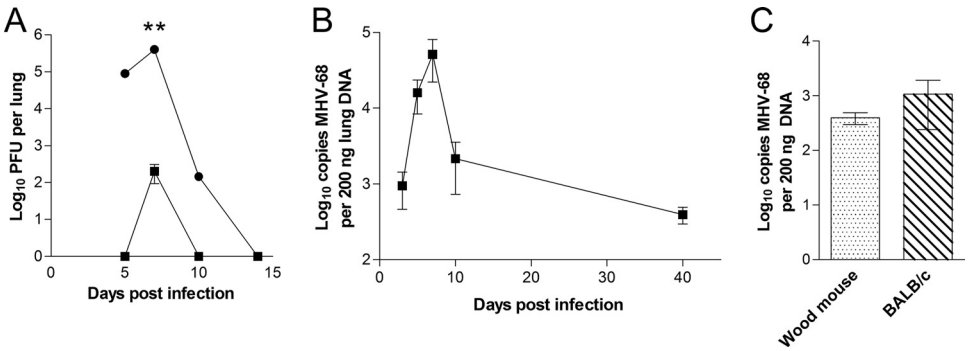

FIG. 1. Virological analysis of infection in the lung. MHV-68 infections of wood mice (■) and BALB/c (●) mice were performed by the intranasal route with 4×10^5 PFU. The error bars represent standard deviations from the mean, and the asterisks represent a statistically significant difference between species (two-way ANOVA with Bonferroni posttests; **, $P < 0.01$). (A) Virus replication in the lung. The data shown are the mean virus titers obtained from four mice per group at each time point and are representative of two independent experiments. (B) Real-time qPCR analysis of the amount of viral DNA present in the lungs of wood mice. The data are presented as $\log_{10}$ copies of viral DNA relative to the amount of cellular *rpl8* DNA present in 200 ng of lung DNA sample analyzed. The data were compiled from analyses of four individual mice at each time point. (C) Real-time qPCR analysis of the amounts of viral DNA present in the lungs of wood and BALB/c mice at day 40 p.i. The data are presented as $\log_{10}$ copies of viral DNA relative to the amount of cellular *rpl8* DNA present in 200 ng of lung DNA sample analyzed. The data were compiled from analyses of four individual mice at each time point.

RESULTS

Wood mouse colony. To assess the pathogenesis of MHV-68 in a natural host, experimental infection of *Apodemus sylvaticus* (wood mouse) was performed and compared to the infection of laboratory mice (strain BALB/c). Wood mice were obtained from a captive-bred colony established at the University of Liverpool (2, 16). At the outset of this study, 20 wood mice were tested both serologically for MHV-68-specific antibodies by ELISA and for the presence of viral DNA by PCR analysis of blood and spleen (3), and all were found to be MHV-68 negative. In addition, each time the animals were infected experimentally, uninfected control mice were likewise analyzed and found to be MHV-68 negative by virus isolation, reactivation, PCR, and serology. The animals in the wood mouse colony were therefore naïve with respect to MHV-68 infection. Analysis of tissues derived from animals in the wood mouse colony by PCR using primers specific for a related herpesvirus that was recently found in a proportion of wood mice (*Apodemus sylvaticus* rhadinovirus 1) (14) was likewise negative, as was analysis by degenerate PCR for herpesvirus DNA polymerase. Thus, the animals were in addition naïve with respect to infection with related herpesviruses. Further, the animals had no other detected infections, as detailed in Materials and Methods. In the experiments presented here, groups of wood and BALB/c mice were infected with MHV-68 via the intranasal route, and three or four animals per species were analyzed at various time points up to 40 days p.i. The data shown are representative of two independent experiments. We chose BALB/c mice, as they have been commonly used as the laboratory host for MHV-68. In addition, there are only minor differences in the pathogenesis of MHV-68 in BALB/c and other strains of *Mus musculus* (e.g., C57BL/6, 129, and CBA), and the time course, virus levels, target cells, and pathology are extremely similar (11, 39–41, 43).

Lower levels of productive virus replication in wood mice. MHV-68 productive infection in lungs was assessed by plaque assay for infectious virus. The results (Fig. 1A) showed that infectious virus was readily recoverable from the lungs of BALB/c mice between days 5 and 10 p.i. In contrast, infectious virus could be consistently detected from the lungs of wood mice only at day 7 p.i. Further, titers of infectious MHV-68 at day 7 p.i. were approximately 3 log units higher in BALB/c than in wood mice ($P < 0.05$). qPCR analysis of viral DNA in the lungs of wood mice revealed an increase to a peak at day 7 p.i., mirroring the profile of infectious virus in BALB/c mice (Fig. 1B). Comparison of viral DNA in the lung at 40 days p.i. (Fig. 1C) demonstrated that wood and BALB/c mice had equivalent loads. Thus, while MHV-68 productive replication peaked at much lower levels in the lungs of wood mice, the two species harbored roughly equivalent levels of viral DNA long term.

Granulomatous infiltrates support virus replication in wood mouse lungs. To further investigate differences between species during acute infection, lungs were harvested from wood and BALB/c mice at various times during the course of infection and examined by histology, by immunohistology to detect MHV-68 structural antigens and cellular markers, and by *in situ* hybridization to detect the MHV-68 viral tRNA-like transcripts (vtRNAs), which are indicative of latent infection (21).

On day 7 p.i., when peak levels of infectious virus were detected in both species, BALB/c mice showed an intense, diffuse increased interstitial cellularity that was dominated by T cells (Fig. 2A and B). There were also numerous necrotic alveolar cells. In addition, leukocyte margination and emigration were observed within blood vessels, along with a macrophage-dominated phlebitis (Fig. 2A). Immunohistological analysis identified viral antigen predominantly in alveolar epithelial cells (Fig. 2C). *In situ* hybridization revealed that viral tRNA was expressed in scattered type II alveolar epithelial cells, lymphocytes, and desquamated alveolar macrophages (Fig. 2D). Other histopathological observations in BALB/c mice (summarized in Table 1) included disseminated small mononuclear infiltrates (macrophages with fewer lymphocytes, mainly T cells), multifocal proliferation/activation of type II pneumocytes, and mild perivascular and peribronchial T- and

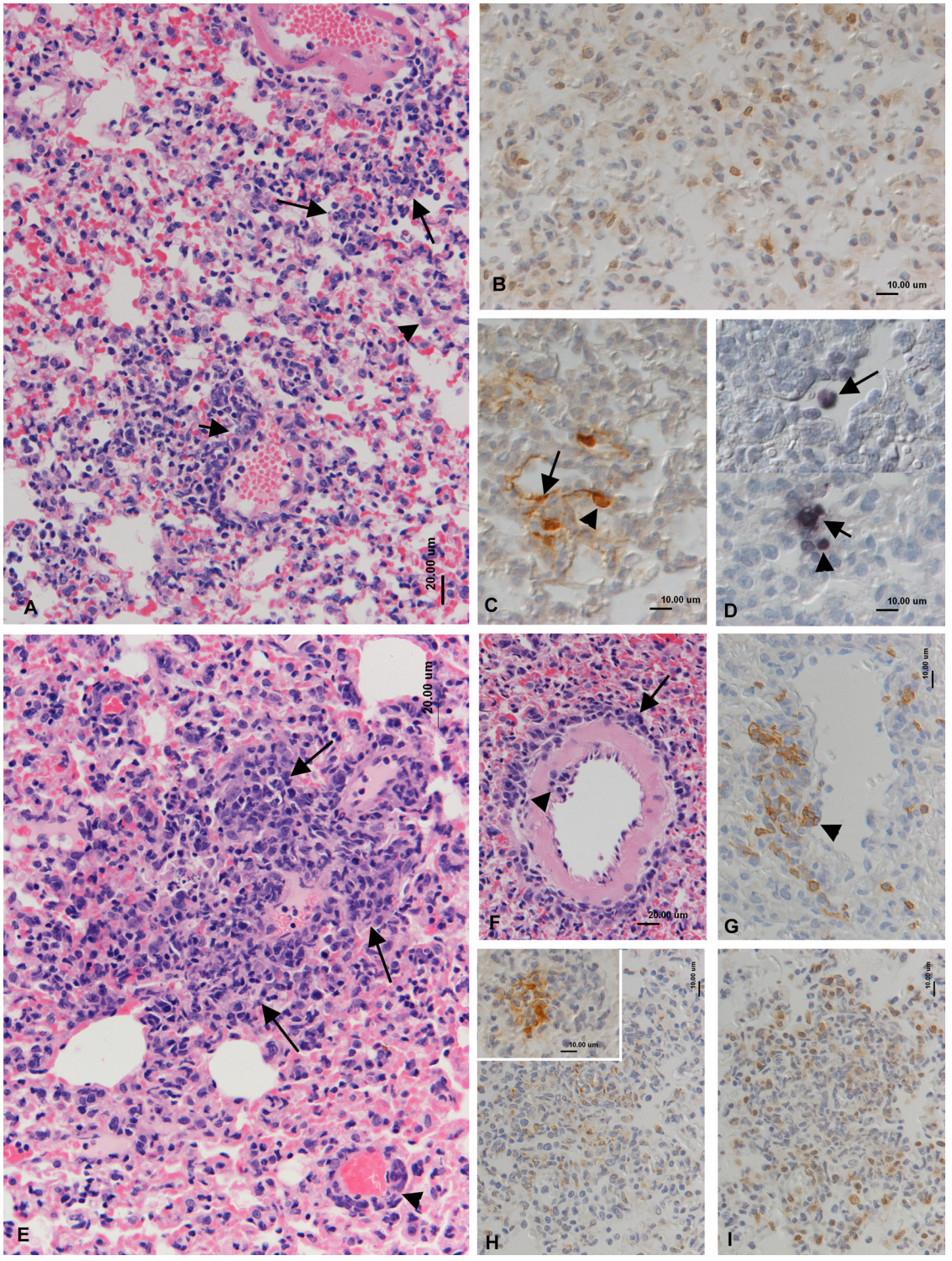

FIG. 2. Histopathological analysis of lungs at day 7 p.i. (A to D) BALB/c mice. (A) Intense diffuse increased interstitial cellularity and small mononuclear infiltrates (large arrows), activation of type II pneumocytes (arrowhead), and mononuclear infiltration of venous wall (phlebitis; small arrow). HE stain. (B) T cells ($CD3^+$; PAP method) dominate in the interstitial infiltration. (C) Viral antigen (PAP method) is expressed by type I (arrow) and type II (arrowhead) pneumocytes. (D) vtRNA expression (RNA-ISH) in a type II pneumocyte (small arrow), a lymphocyte (arrowhead), and a desquamed alveolar macrophage (large arrow). (E to I) Wood mice. (E) Multifocal granulomatous infiltration (arrows) and perivenous lymphocyte infiltration (arrowhead). HE stain. (F) Artery with emigrating (arrowhead) and perivascular (arrow) lymphocytes. HE stain. (G) B cells ($CD45R^+$; ABC method) dominate in the perivascular infiltrate and are seen rolling and attached to endothelial cells (arrowhead). (H) Staining for lysozyme (PAP method) identifies numerous macrophages in the focal granulomatous infiltrates. (Inset) Viral antigen is detected (PAP method) in macrophages within the granulomatous infiltrates. (I) T cells ($CD3^+$; PAP method) represent the dominant lymphocyte population in granulomatous infiltrates.

TABLE 1. Summary of key histological findings in the lung after intranasal MHV-68 infection

Day p.i.	Assay	Histological finding (level of intensity)[a]	
		BALB/c mice	Wood mice
7	HE[b]	Intense increased cellularity (+++) Necrosis of AEC (++) Monocyte/macrophage phlebitis (++) Perivascular LC cuffing (+)	Diffuse increased cellularity (++) Necrosis of AEC (+) Multifocal granulomatous infiltrations (++) Perivascular/peribronchial LC cuffing (+++)
	MHV-68 antigen	Disseminated AEC (type I and II) and entire alveoli (++)	Disseminated AEC and entire alveoli Often, macrophages within granulomatous infiltrates (++)
	B cell	Perivascular accumulations (+) Interstitial accumulations (+)	Major cell type in perivascular/peribronchial LC cuffing (+++) Rolling/emigrating cells
	T cell	Perivascular accumulations (+) Interstitial accumulations (+)	Perivascular accumulations (+) Granulomatous infiltrates (++)
	Lysozyme	Disseminated macrophages and phlebitis	Granulomatous infiltrates (++)
	RNA-ISH (vtRNA)	Scattered AEC (+) Occasional LC (+)	Very few AEC (+)
14	HE	Diffuse increased cellularity (++) Necrosis of AEC (++) Focal granulomatous infiltrations (+)	Diffuse increased cellularity (+) Necrosis of AEC (+) Multifocal granulomatous infiltrations (++) Perivascular/peribronchial LC cuffing (+++)
	MHV-68 antigen	Negative	Occasionally with in Perivascular/peribronchial LC (+) Granulomatous infiltrates (+)
	B cell	Diffuse cellularity (++)	Perivascular/peribronchial LC within iBALT (+++) Perivascular/peribronchial LC within inflammation response (+++)
	T cell	Diffuse cellularity and focal inflammation response (+++)	Perivascular/peribronchial LC within inflammation response (+)
	Lysozyme	Numerous alveolar macrophages (desquamated) (+++)	Macrophages within focal infiltrates (+) FDC within iBALT (+)
	PCNA		Within cells of iBALT (+)
	RNA-ISH (vtRNA)	Negative	Numerous LC within iBALT (++)
21	HE	Diffuse increased cellularity (++) Small focal LC accumulations (+)	Diffuse increased cellularity (+) Necrosis of AEC (+) Multifocal granulomatous infiltrations (+) Perivascular/peribronchial LC cuffing (++)
	MHV-68 antigen	Negative	Negative
	B cell	Disseminated (++)	Numerous within parenchyma and LC accumulations (++)
	T cell	Disseminated and within small accumulations (++)	Disseminated and occasionally within LC accumulations (+)
	Lysozyme	Numerous disseminated alveolar macrophages (++)	Scattered macrophages in granulomatous infiltrates (+)
	RNA-ISH (vtRNA)	Negative	Negative
40	HE	Very mild perivascular/peribronchial LC accumulations (+)	Very mild perivascular/peribronchial LC accumulations (+)

[a] Level of intensity: +, mild; ++, moderate; +++, intense/severe. AEC, alveolar epithelial cell; LC, lymphocyte(s).
[b] HE, hematoxylin and eosin.

B-cell infiltrations. These observations are consistent with interstitial pneumonitis in BALB/c mice caused by MHV-68.

In contrast, on day 7 p.i., wood mice exhibited only mild, diffuse increased interstitial cellularity with T and B cells in equivalent amounts. Necrotic alveolar cells were seen but were less numerous than in BALB/c mice. Mild to moderate mononuclear perivascular and peribronchial infiltration was observed (Fig. 2E to G). Interestingly, this consisted predominantly of B cells (Fig. 2G), with scattered macrophages and very few T cells (not shown). B cells were also seen attached to the endothelium, rolling and emigrating from vessels (Fig. 2G). Both the B-cell-rich infiltration and emigrating B cells were negative for viral antigen and vtRNA (not shown). A separate, prominent feature in the lungs at day 7 p.i. was multifocal granulomatous infiltration (Fig. 2E). These infiltrates consisted mainly of macrophages and T cells (Fig. 2H and I). Viral antigen was detected in alveolar epithelial cells and macrophages within the granulomatous infiltrates (Fig. 2H, inset), whereas vtRNA was found in only a single alveolar epithelial cell (not shown). Granulomatous infiltrates were still detectable up to 28 days p.i., albeit in decreasing size and numbers. Interestingly, viral antigen was detected occasionally within

epithelial cells and macrophages in these infiltrates up to 14 days p.i. (not shown). The histopathological findings are summarized in Table 1.

Viral latency in iBALT. On day 14 p.i., BALB/c mice exhibited an inflammatory infiltrate in the lung that was less intense than at day 7 and that consisted mainly of numerous disseminated lymphocytes (Fig. 3A), which were predominantly T cells (not shown). In addition, there were numerous (desquamed) alveolar macrophages (Fig. 3A and B). Neither viral antigen nor vtRNA was found, consistent with the resolution of virus productive infection in the lung at or before this time point in BALB/c mice.

A major finding in wood mice at this time point was an intense perivascular and peribronchiolar lymphocyte-dominated infiltration. In contrast to the B-cell predominance seen at day 7 p.i., this infiltration now contained T and B cells in similar proportions (Fig. 3C to E). B cells were also numerous within blood vessel lumina (Fig. 3D) and were seen attached to the endothelium and emigrating from veins. In addition to the perivascular/peribronchiolar infiltration described above, distinct focal, follicle-like lymphocyte accumulations containing germinal centers were present with a peribronchiolar and perivascular distribution. These differed in that they were almost entirely composed of B cells (Fig. 3F, H, and I). Many lymphocytes in these accumulations expressed vtRNA (Fig. 3G) but did not express viral antigen (not shown), indicative of a latent infection. The germinal centers were comprised of large lymphoblasts with a few large, faintly lysozyme-positive FDC-like cells (Fig. 3J) and a few scattered T cells (not shown). Detection of PCNA expression in many cells revealed that local cell proliferation was occurring (Fig. 3J). It was concluded, therefore, that these focal, follicular-like accumulations were iBALT. The interstitium had a mild diffuse increased cellularity with T and B cells in equivalent numbers, as well as small focal mononuclear cell infiltrations and occasional type II pneumocyte proliferation/activation (not shown).

The pathological alterations in BALB/c mice through day 40 p.i. were similar to those seen at up to 14 days p.i. but decreased in intensity over time. Neither viral antigen nor vtRNA expression was detected in BALB/c mice after 10 days p.i. The perivascular and peribronchiolar lymphocyte accumulations seen in wood mouse lungs persisted through 40 days p.i. but decreased greatly in size. Neither vtRNA nor antigen was detected after 14 days p.i., and iBALT began to subside after 14 days p.i. (Table 1).

Splenic latency in the absence of marked leukocytosis and splenomegaly. Splenomegaly as a result of a transient rise in leukocyte number within the spleen is characteristic of MHV-68 infection of laboratory mice (25, 40). However, after infection of wood mice, there was no observable increase in spleen size at any time point. To determine if a less prevalent leukocytosis occurs in this host, total leukocyte numbers in the spleen were determined for infected wood and BALB/c mice at various times p.i. The spleens of uninfected wood mice were much smaller than those of BALB/c mice and generally contained on the order of 10^7 leukocytes compared to ca. 10^8 in BALB/c mice. As can be seen in Fig. 4A, infection in BALB/c mice induced the typical increase (2.6-fold) in spleen cell numbers, which peaked at day 14 and returned to normal 28 to 40 days p.i. Following infection of wood mice, a more modest 1.4-fold increase in spleen cell numbers was observed, which also peaked at day 14 but returned to normal or below by day 20 p.i.

To assess the number of latently infected cells in the spleen, an infective-center assay was performed. Infective centers were detected in BALB/c mice from day 7 p.i. onward, with the peak in latency coinciding with the peak in leukocytosis at 14 days p.i., as expected (Fig. 4B). The same general profile was observed in the spleens of MHV-68-infected wood mice, revealing that latency was achieved as efficiently in this natural host. In fact, the peak level of latency (14 days p.i.) in the spleens of wood mice was significantly higher ($P < 0.01$) than in BALB/c mice. To discount the possibility that scored infective centers were a result of preformed virus particles (and therefore not indicative of reactivated latent virus), splenocytes were exposed to three freeze-thaw cycles prior to being plated onto NIH 3T3 cells. In a small number of samples, infectious virus was detected, but it was always less than 10 PFU per spleen and was subtracted from the final infective-center numbers (Fig. 4B).

The results of infective-center analysis were confirmed by qPCR analysis for viral DNA in the spleen, which revealed similar profiles of infection at various times p.i. (Fig. 4C). Also, in concordance with results from the infectious-center assay, a significantly higher level of MHV-68 DNA was observed at 14 days p.i. in the wood mouse ($P < 0.05$). In addition, in both species, there was persistence of viral DNA long term (40 days p.i.) (Fig. 4C). Although there appeared to be a lower level of both infectious centers and viral DNA in wood mice at later times postinfection, up to 40 days p.i. (Fig. 4B and C), the differences were not statistically significant.

To shed further light on these differences, spleens of infected BALB/c and wood mice were examined by histology, immunohistology, and *in situ* hybridization. On day 7 p.i., spleens were generally unaltered, and neither viral antigen nor vtRNA was detected. On day 14 p.i. within infected BALB/c mice, the white pulp was composed of large, cell-rich, and poorly delineated follicles and large T-cell zones (Fig. 5A). Compared to uninfected animals, the red pulp showed increased cellularity, with macrophages predominating (ca. 50%) and forming perifollicular rims (Fig. 5B). Other cell types in the red pulp, many of which were PCNA positive (proliferating), included B cells (ca. 30%) and T cells (ca. 20%) (not shown). Follicles exhibited numerous FDCs and tingible body macrophages (Fig. 5C), as well as numerous mitotic cells and scattered apoptotic cells, indicative of high cell turnover. Germinal centers were not obvious, but numerous PNA-positive (germinal-center) B cells were present, forming nondelineated accumulations in follicle centers (not shown). Germinal-center cells were also PCNA positive (not shown). MHV-68 antigen was not detected, but vtRNA was observed in variable numbers of cells within the follicles and appeared to be randomly distributed (Fig. 5D).

In contrast to BALB/c mice, infected wood mice at day 14 p.i. had smaller, moderately sized, distinctly delineated splenic follicles, often with germinal centers (Fig. 5E) and high cellular turnover (numerous mitotic and apoptotic cells). T-cell zones were relatively small, and the red pulp was of only moderate cellularity compared to BALB/c mice. Besides B cells (ca. 30%) and T cells (ca. 10%) (not shown), macro-

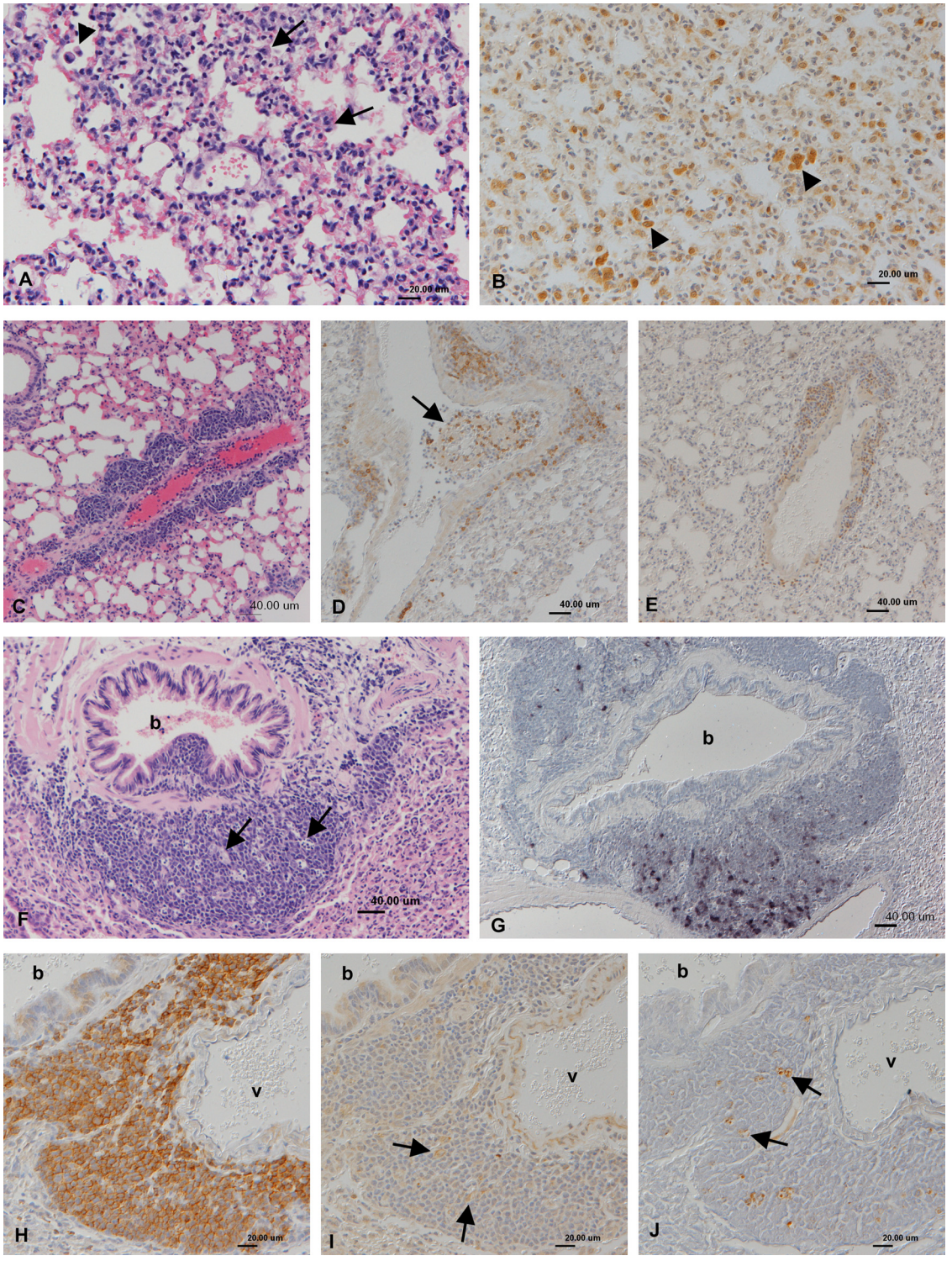

FIG. 3. Histopathological analysis of lungs at day 14 p.i. (A and B) BALB/c mice. (A) Moderate diffuse increased interstitial cellularity, activation of type II pneumocytes (arrow), and desquamation of cells into alveolar lumen (arrowhead). HE stain. (B) Staining for lysozyme (PAP method) highlights the presence of numerous alveolar macrophages and identifies the desquamed cells as macrophages (arrowheads). (C to J) Wood mice. (C) Moderate perivascular lymphocyte infiltration. HE stain. (D) B cells ($CD45R^+$; ABC method) are numerous in the perivascular infiltrate and are found in large numbers in the vessel lumen (arrow). (E) T cells ($CD3^+$; PAP method) are equally numerous in the perivascular infiltrate. (F) Peribronchial, follicle-like lymphocyte accumulation with germinal center containing tingible body macrophages (arrows). HE stain. (G) vtRNA (RNA-ISH) is expressed by numerous lymphocytes in the follicle-like peribronchial lymphocyte accumulation. (H) Peribronchial lymphocyte accumulations are almost entirely composed of B cells ($CD45R^+$; ABC method). (I) Staining for lysozyme (PAP method) highlights follicular dendritic cells (arrows) within the follicles. (J) Staining for PCNA (PAP method) identifies proliferating cells (arrows) in the follicles. b, bronchial lumen; v, blood vessel lumen.

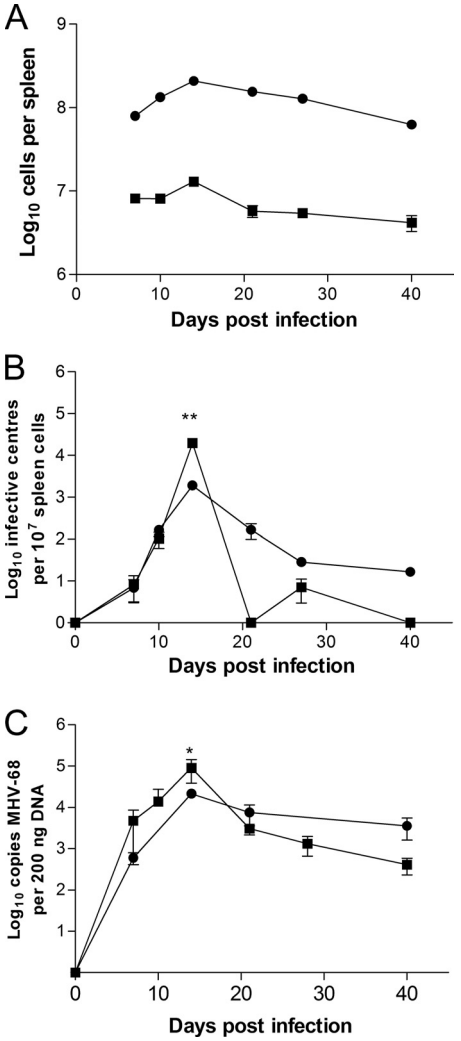

FIG. 4. Virological analysis of infection of the spleen. MHV-68 infections of wood (■) and BALB/c (●) mice were performed by intranasal inoculation with 4×10^5 PFU. The error bars represent standard deviations from the mean, and the asterisks represent a statistically significant difference between species at the indicated time points (two-way ANOVA with Bonferroni posttests; **, $P < 0.01$; *, $P < 0.05$). (A) Total spleen cell numbers within infected mice; shown are the mean cell numbers obtained from four infected animals per group at each time point. (B) Latently infected cells in the spleens of infected wood and BALB/c mice as determined by infective-center assay; the data from four animals per group are shown at each time point. Less than 10 PFU from preformed infectious virus was detected in freeze-thaw lysates, and this value was subtracted from the total infective centers, when observed. (C) qPCR analysis of the amounts of viral DNA present in the spleens of wood and BALB/c mice; the data are presented as $\log_{10}$ copies of viral genomes relative to the amount of cellular *rpl8* DNA present in the sample (200 ng). The data were compiled from analyses of four individual mice at each time point.

phages were the most numerous in the red pulp (Fig. 5F). Viral antigen was expressed by variable numbers of macrophages in the red pulp (notably those located around follicles) and also occasionally in tingible body macrophages within follicles (Fig. 5G). Identification of germinal centers was attempted using PNA staining, as in BALB/c mice, but in wood mice this failed. To circumvent this, PCNA staining was used, which revealed a high number of cells within germinal centers of follicles undergoing high cellular proliferation (not shown). We therefore concluded that germinal-center cells were present but that PNA was unable to bind due to subtle species differences between BALB/c and wood mice. vtRNA was detected in variable numbers of lymphocytes/lymphoblasts within follicle centers (Fig. 5H) and occasional lymphocytes and macrophages in the red pulp.

Wood mice mount a stronger neutralizing-antibody response. Due to the apparent differences in the B-cell reactions during MHV-68 infection found between BALB/c and wood mice, we next investigated the production of antibody to MHV-68. Sera taken at various times p.i. were analyzed by ELISA for MHV-68-specific antibody and by a plaque reduction assay to determine the titers of neutralizing antibodies. In both species, the titers of anti-MHV-68 antibodies rose sharply and peaked at day 14, declining slightly through 21 days p.i. (Fig. 6A). At day 40 p.i., the respective titers remained similar to those at day 21 but were lower in wood mice than in BALB/c mice ($P < 0.05$). Neutralizing antibody in BALB/c mice was detectable at 7 days p.i., but antibody levels did not rise significantly throughout the course of the infection, monitored through 40 days p.i. (Fig. 6B). Surprisingly, the levels of neutralizing antibody in wood mice not only rose more sharply, but titers were significantly higher than in BALB/c mice at days 14 ($P < 0.01$) and 40 ($P < 0.01$) p.i.

DISCUSSION

The experimental infection of inbred strains of laboratory mice (*Mus musculus*) with MHV-68 has become an attractive small-animal model for the study of gammaherpesvirus pathogenesis (25, 39, 40). Here, we have described the first investigation of MHV-68 pathogenesis in a natural host, the wood mouse (*Apodemus sylvaticus*). In our comparative analysis of infection of BALB/c and wood mice, we noted significant differences associated with MHV-68 infection in two organs—lung and spleen—that are primary sites of acute and persistent infection. While MHV-68 infection was comparatively assessed in only BALB/c mice here, previous studies have found only minor differences in virus loads, pathogenesis, and host response in BALB/c mice relative to other inbred strains (e.g., 129 and C57BL/6) after infection with MHV-68 (8, 39). Thus, we feel that our observations and conclusions will extend to other commonly used inbred strains of *M. musculus*.

While inoculation of BALB/c and wood mice with MHV-68 via the intranasal route resulted in productive virus replication with similar kinetics in the lungs of both species, substantially (ca. 3 log units) less infectious virus could be recovered from the lungs of wood mice. Indeed, the only time point at which virus was readily detected in wood mice by standard plaque assay was at day 7 p.i. Despite this, viral-antigen expression persisted in alveolar epithelia and macrophages within inflammatory infiltrates of wood mice (but not BALB/c mice) through 14 days p.i., and the levels of viral DNA in lungs were equivalent in both species of mice at day 40 p.i. Thus, the lower level of replication observed in wood mice following primary infection is more than sufficient to establish a persistent (latent) infection in this host.

The basis for restricted MHV-68 replication in the lungs of

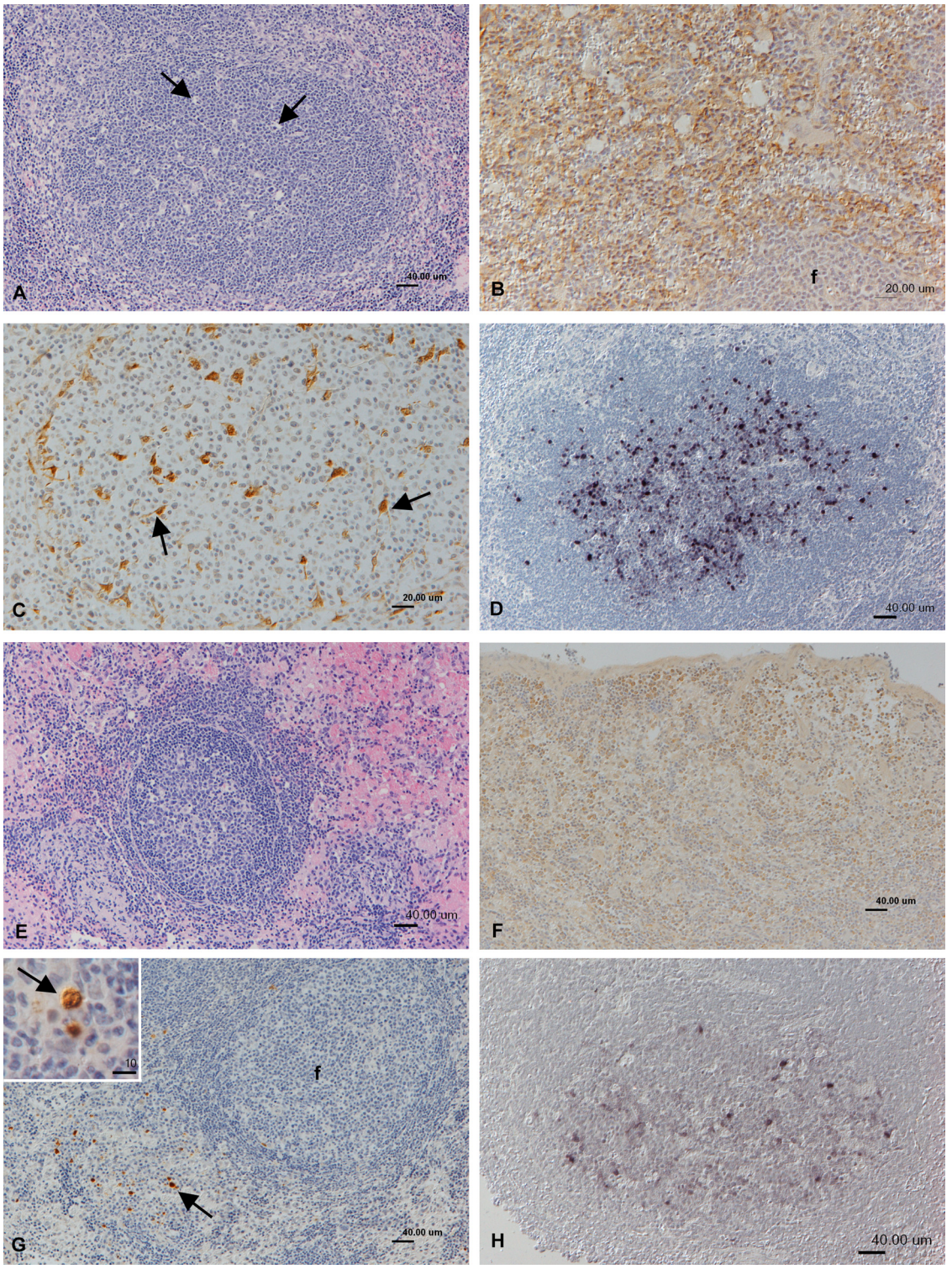

FIG. 5. Histopathological analysis of spleens at day 14 p.i. (A to D) BALB/c mice. (A) The white pulp is composed of large, cell-rich, poorly delineated follicles with numerous tingible body macrophages (arrows). HE stain. (B) In the cell-rich red pulp, macrophages ($F4/80^+$; ABC method) dominate. f, follicle. (C) Lysozyme staining (PAP method) identifies numerous follicular dendritic cells (arrows) and tingible body macrophages within follicles. (D) vtRNA (RNA-ISH) expression is detected in numerous randomly distributed lymphocytes. (E to H) Wood mice. (E) The white pulp is composed of moderately sized, well-delineated follicles with germinal centers. HE stain. (F) The red pulp is moderately cell rich; macrophages dominate ($F4/80^+$; ABC method). (G) Viral antigen (PAP method) is detected in macrophages in the red pulp (arrow) and occasionally in tingible body macrophages within follicles (inset; arrow). f, follicle. (H) vtRNA (RNA-ISH) is detected in lymphocytes within the germinal center.

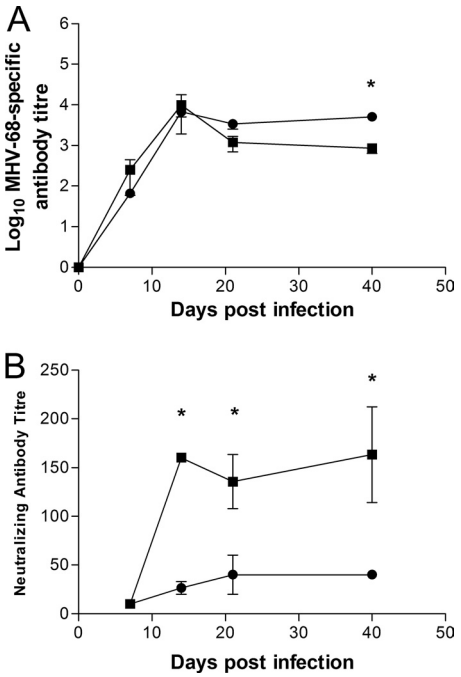

FIG. 6. Anti-MHV-68 antibody levels in infected animals. MHV-68 infection of wood (■) and BALB/c (●) mice was performed intranasally with 4×10^5 PFU. The asterisks indicate a statistically significant difference between species at the indicated time points (two-way ANOVA with Bonferroni posttests; $P < 0.01$). (A) Total anti-MHV-68 antibody titers were measured by ELISA. Each data point represents the $\log_{10}$ mean reciprocal dilution at which samples became negative (cutoff dilution = mean absorbencies of all preimmune sera samples + 2 standard deviations) ± the standard error of the mean. The graph is representative of 3 individual experiments. *, $P < 0.01$. (B) MHV-68 neutralizing-antibody titers as measured by plaque reduction assay. The reciprocal of the dilution that resulted in 50% reduction of the number of MHV-68 plaques (compared to a preimmune serum incubated with MHV-68) was plotted. Each time point represents serum samples from 4 MHV-68-infected BALB/c or wood mice ± the standard error of the mean.

wood mice is unclear but is likely to be a function of a more appropriate host response in the wood mouse than in the laboratory host. This could be due to better evolutionary adaptation by a natural host species. However, laboratory model host strains of mice (BALB/c, C57BL/6, 129, and CBA) are highly inbred and consequently may be deficient in critical host response functions (8). Examples of this are the Mx1 protein, mediating resistance to influenza viruses, which is absent in many inbred strains (35), and the major histocompatibility complex (MHC) and NK cell gene complex loci that encode resistance to murine cytomegalovirus (34). Further analysis using captive-bred, outbred *Mus musculus* will be required to draw firm conclusions.

There was not only a quantitative difference in the productive infection in lungs between wood and BALB/c mice, but also a dramatic qualitative difference in terms of pathological changes. In BALB/c mice, the most prominent features associated with primary infection are interstitial pneumonitis, with virus replication in alveolar epithelial cells, and a diffuse interstitial mononuclear (mainly T) cell infiltration. Similar changes were seen in C57BL/6 mice (not shown). In contrast, acute MHV-68 infection of wood mice resulted in three parallel pathological features within the lung: (i) virus replication was predominantly contained in focal granulomatous infiltrations, (ii) perivascular and peribronchial B lymphocyte recruitment occurred early during infection, and (iii) germinal-center and iBALT formation occurred, peaking approximately 14 days p.i. and containing many latently infected B lymphocytes.

In BALB/c mice, while monocyte/macrophage involvement is an aspect of the inflammatory response in the lungs, antigen-positive pneumocytes and a diffuse interstitial T-cell response predominate (40). These observations in BALB/c mice were corroborated during the present study (Fig. 2A and B and 3A and B). In contrast, the predominant pathological feature in the lungs of wood mice at day 7 p.i. was a multifocal granulomatous infiltration containing macrophages that expressed viral antigen and, to a lesser degree, T cells (Fig. 2E to I), which was correlated with the peak in infectious virus production.

Granulomas are highly organized structures characterized by the presence of differentiated macrophages that act as contained immune environments to "wall off" an infecting organism. *Mycobacterium* spp. are the most intensely studied infectious agents that characteristically induce granuloma formation in the lungs (20), which serves to limit bacterial replication. It is postulated that the bacteria, upon introduction into the respiratory tract, first encounter alveolar macrophages, which in turn promote the recruitment of monocytes and their differentiation into activated macrophages that upregulate the production of gamma interferon (IFN-γ) and interleukin 12 (IL-12), cytokines important for induction of a granulomatous inflammation.

Although the presence of granulomatous infiltrates may explain why significantly reduced titers of virus were recovered from wood mouse lungs, we find it intriguing that viral antigen is strongly expressed in macrophages within these infiltrates (Fig. 2H), suggesting that they may actually act as foci of virus production during acute infection. Although granuloma formation is an effective immune response to limit bacterial replication, it has been discovered that *Mycobacterium* spp. actively induce their formation (20). It is certainly possible that pathogenesis-related proteins of MHV-68, such as the chemokine-binding protein M3 (6, 45), might contribute to focal granulomatous infiltrations in the lung by promoting the recruitment of macrophages from the blood. Further, the induction of granulomatous infiltrates by viral proteins of the lytic cycle may provide a strong source of chemokines involved in the formation of iBALT or the activation of endothelial cells for the extravasation of B cells, which appear to benefit the virus in terms of the establishment of a persistent latent infection (see below).

In light of our findings, it is notable that KSHV infection is also associated with a granulomatous/lymphocytic interstitial lung disease in patients with common variable immunodeficiency (47). Here, as in infected wood mice, virus antigen-positive lymphocytes are present in interstitial foci within the lung. The development of such lesions may therefore be a common feature of pathogenesis associated with this group of viruses, and further study of MHV-68 in wood mice may thus provide valuable insight into KSHV-related disease in the lung.

Recruitment of B cells to form perivascular and peribronchiolar accumulations in the lung was observed in wood mice as early as 7 days p.i. (Fig. 2F and G). While cell recruitment

was also seen in BALB/c mice, it primarily involved T cells (Fig. 2B). In wood mice, virus-negative B cells were seen rolling along endothelial walls and emigrating from the vessels (Fig. 2G). By day 14 p.i., these perivascular/bronchiolar accumulations had enlarged and developed into two distinct types: one that contained B and T lymphocytes in similar numbers (Fig. 3C to E), and the other iBALT, characterized as focal, follicle-like accumulations that were B-cell rich and contained germinal centers (Fig. 3F to J) comprised of large lymphoblasts with scattered FDC-like cells and evidence of cellular proliferation. At day 14 p.i., both the perivascular/peribronchiolar accumulations and iBALT contained latently infected lymphocytes, i.e., vtRNA positive, viral structural antigen negative.

The extravasation of leukocytes (seen at day 7 and continuing through day 14 p.i.) in this way is typically due to activated endothelial cells expressing adhesion molecules and chemokines on their surfaces. Once leukocytes have passed through the endothelial wall, they migrate to the site of infection via chemokine gradients. This response could be either induced or facilitated by MHV-68. The fact that the cells observed interacting with vessel walls were specifically B cells suggests a viral influence. The MHV-68 chemokine-binding protein M3 binds to and inhibits a broad range of chemokines but selectively does not inhibit B-cell-associated chemokines (30, 44) (unless expression is forced in transgenic mice [26]), and could possibly have an influence in this process. Indeed, we have recently determined that these features associated with MHV-68 infection specifically in the lungs of wood mice require the expression of M3 (D. J. Hughes, A. Kipar, J. T. Sample, and J. P. Stewart, unpublished observation).

In contrast to BALB/c mice, there was significant latent infection in wood mouse lungs (predominantly in lymphocytes) that peaked around 14 days p.i., suggesting that in the natural host, there is considerable local expansion of the latently infected B-cell population in the lung during primary infection. Interestingly, latently infected lymphocytes are not evident in lungs after day 14 p.i. Though the fate of these lymphocytes is currently unclear, they may go on to seed latency in other organs, which may be particularly critical in the context of a natural infection where the output of infectious virus is low at the primary site of infection.

Unlike for other species, the presence of classical constitutive BALT (cBALT) is controversial in laboratory mice, which appear not to generate BALT independently of antigen. Pathogens, such as influenza virus, however, can rapidly promote within mice devoid of secondary lymphoid organs the formation of iBALT that is capable of priming virus-specific T and B cells (27). It is likely that in normal mice, iBALT formation, which is delayed relative to the immune response in draining lymph nodes, is obscured (27). Unlike the cBALT seen in other species, iBALT in mice is not only found in upper bronchi, but is also perivascular, peribronchial, and even within interstitial spaces in the lower airways (27). The development of iBALT in the wood mouse in the absence of an underlying genetic mutation, therefore, is unusual for a rodent. Thus, MHV-68 infection of wood mice could provide an excellent model with which to study natural iBALT formation and function.

Upon replication in the lungs of laboratory mice, MHV-68 traffics to the spleen, which serves as a major reservoir of latent virus thereafter (17, 19, 22, 46, 48). Characteristically, in laboratory mice, this results in splenic mononucleosis, in which a transient increase in the number of leukocytes leads to splenomegaly (25, 40). This response has been studied in some detail in laboratory strains of mice, where it is dependent on MHV-68-infected B cells (43) and on $CD4^+$ T cells (7, 42). In contrast, infection of wood mice did not result in significant splenomegaly, but the transient spike in latently infected splenocytes peaking at 14 days p.i., followed by maintenance of long-term latency in this host, was similar to that seen in BALB/c mice. Thus, splenomegaly is not a pathological feature of infection in wood mice, and it is not required for long-term latency. This is analogous to natural infection with EBV, where only a proportion of those infected suffer infectious mononucleosis and it is not a requirement for the establishment of long-term viral latency.

Histologically, the spleen responded very differently to infection in BALB/c and wood mice. In BALB/c mice at 14 days p.i., the B-cell follicles were very large and densely packed, but secondary follicle formation was not apparent even though proliferating germinal-center B cells could be detected. Well-delineated secondary follicle formation was, however, evident at day 21 p.i., and latently infected cells appeared to be randomly distributed throughout the follicles. In fairly stark contrast, within wood mouse spleens at day 14 p.i., distinct germinal centers were obvious, with well-delineated secondary follicle formation (a light zone within the germinal center), and *in situ* hybridization analysis revealed that latent virus was strictly contained within these germinal centers. Moreover, the germinal-center reaction in wood mice was prolonged and still evident, albeit to a lower degree, between 21 and 28 days p.i. Interestingly, viral antigen was still being expressed in macrophages in the red pulp after 14 days p.i. in wood mice, whereas this was not observed in BALB/c mice. It is quite possible that these antigen-expressing macrophages provide the signal for a prolonged germinal-center reaction.

The antibody response to gammaherpesvirus infections has been well characterized, including the response to MHV-68 infection in laboratory mice. Although virus-specific antibody is important for long-term control of MHV-68 (38), the antibody response to lytic infection in these hosts appears to be inferior. In the first week following infection, IgM antibodies are detectable, after which a massive $CD4^+$ T-cell-dependent polyclonal-antibody response ensues (dominated by IgG2a and IgG2b), a large proportion of which is not able to neutralize purified MHV-68 (33, 36). Consistent with this, titers of neutralizing antibody in BALB/c mice were not significant until 21 days p.i. and remained low but constant throughout the course of the infection. It has also been shown previously that upon secondary MHV-68 infection of laboratory mice, there is no significant boost in neutralizing antibody (37). In wood mice, in contrast, the levels of neutralizing antibody rose sharply, and at day 14 p.i., titers were significantly higher than in BALB/c mice. The level of neutralizing antibody in serum then remained, up to day 40 p.i., largely the same as it was at day 14, significantly higher than in BALB/c mice. Although the basis for these dramatic differences in neutralizing-antibody production is unclear, it is possible that the apparently stronger germinal-center reaction in infected wood mouse spleens is responsible.

In summary, human gammaherpesviruses are significant pathogens linked to numerous malignant or lymphoproliferative diseases. Unfortunately, due to their narrow host range, it is very difficult to investigate their pathogenesis; hence, the development of small-animal models is critical. Previous work in which human gammaherpesviruses were used to infect nonhuman hosts proved inconclusive, and work with homologous simian gammaherpesviruses in their natural hosts highlighted the importance of using appropriate host models to study pathogenesis. The numerous differences we have observed during this study further reinforce this notion. Since wood mice are a natural host for MHV-68, this is an attractive alternative system with which to study gammaherpesvirus pathogenesis. In particular, its use may shed further light on the functions of unique genes in the induction and modification of the host's response to these viruses and potentially reveal how the virus is transmitted to the naïve host.

ACKNOWLEDGMENTS

This work was supported by a Royal Society (London) University Research Fellowship (to J.P.S.), U.S. Public Health Service grant CA090208, and Cancer Center Support Grant CA21765 from the National Cancer Institute; the American Lebanese Syrian Associated Charities (ALSAC); and the Penn State Hershey Cancer Institute.

We thank Malcolm Bennett, Department of Veterinary Pathology, University of Liverpool, for help, advice, and generous access to the wood mouse colony.

The authors have no financial conflicts of interest.

REFERENCES

1. **Becker, S. D., M. Bennett, J. P. Stewart, and J. L. Hurst.** 2007. Serological survey of virus infection among wild house mice (*Mus domesticus*) in the UK. Lab. Anim. **41:**229–238.
2. **Bennett, M., A. J. Crouch, M. Begon, B. Duffy, S. Feore, R. M. Gaskell, D. F. Kelly, C. M. McCracken, L. Vicary, and D. Baxby.** 1997. Cowpox in British voles and mice. J. Comp. Pathol. **116:**35–44.
3. **Blasdell, K., C. McCracken, A. Morris, A. A. Nash, M. Begon, M. Bennett, and J. P. Stewart.** 2003. The wood mouse is a natural host for Murid herpesvirus 4. J. Gen. Virol. **84:**111–113.
4. **Blaskovic, D., M. Stancekova, J. Svobodova, and J. Mistrikova.** 1980. Isolation of five strains of herpesviruses from two species of free living small rodents. Acta Virol. **24:**468.
5. **Bowden, R. J., J. P. Simas, A. J. Davis, and S. Efstathiou.** 1997. Murine gammaherpesvirus 68 encodes tRNA-like sequences which are expressed during latency. J. Gen. Virol. **78:**1675–1687.
6. **Bridgeman, A., P. G. Stevenson, J. P. Simas, and S. Efstathiou.** 2001. A secreted chemokine binding protein encoded by murine gammaherpesvirus-68 is necessary for the establishment of a normal latent load. J. Exp. Med. **194:**301–312.
7. **Brooks, J. W., A. M. Hamilton-Easton, J. P. Christensen, R. D. Cardin, C. L. Hardy, and P. C. Doherty.** 1999. Requirement for CD40 ligand, CD4(+) T cells, and B cells in an infectious mononucleosis-like syndrome. J. Virol. **73:**9650–9654.
8. **Brownstein, D. G.** 1998. Comparative genetics of resistance to viruses. Am. J. Hum. Genet. **62:**211–214.
9. **Bruce, A. G., A. M. Bakke, H. Bielefeldt-Ohmann, J. T. Ryan, M. E. Thouless, C. C. Tsai, and T. M. Rose.** 2006. High levels of retroperitoneal fibromatosis (RF)-associated herpesvirus in RF lesions in macaques are associated with ORF73 LANA expression in spindleoid tumour cells. J. Gen. Virol. **87:**3529–3538.
10. **Clarke, J. R.** 1999. Voles, p. 331–334. *In* T. B. Poole (ed.), UFAW handbook on the care and management of laboratory animals, vol. 1. Blackwell Scientific, Oxford, United Kingdom.
11. **Dutia, B. M., C. J. Clarke, D. J. Allen, and A. A. Nash.** 1997. Pathological changes in the spleens of gamma interferon receptor-deficient mice infected with murine gammaherpesvirus: a role for CD8 T cells. J. Virol. **71:**4278–4283.
12. **Efstathiou, S., Y. M. Ho, and A. C. Minson.** 1990. Cloning and molecular characterization of the murine herpesvirus 68 genome. J. Gen. Virol. **71:** 1355–1364.
13. **Ehlers, B., G. Dural, N. Yasmum, T. Lembo, B. de Thoisy, M. P. Ryser-Degiorgis, R. G. Ulrich, and D. J. McGeoch.** 2008. Novel mammalian herpesviruses and lineages within the Gammaherpesvirinae: cospeciation and interspecies transfer. J. Virol. **82:**3509–3516.
14. **Ehlers, B., J. Kuchler, N. Yasmum, G. Dural, S. Voigt, J. Schmidt-Chanasit, T. Jakel, F. R. Matuschka, D. Richter, S. Essbauer, D. J. Hughes, C. Summers, M. Bennett, J. P. Stewart, and R. G. Ulrich.** 2007. Identification of novel rodent herpesviruses, including the first gammaherpesvirus of Mus musculus. J. Virol. **81:**8091–8100.
15. **Ehtisham, S., N. P. Sunil-Chandra, and A. A. Nash.** 1993. Pathogenesis of murine gammaherpesvirus infection in mice deficient in CD4 and CD8 T cells. J. Virol. **67:**5247–5252.
16. **Feore, S. M., M. Bennett, J. Chantrey, T. Jones, D. Baxby, and M. Begon.** 1997. The effect of cowpox virus infection on fecundity in bank voles and wood mice. Proc. R. Soc. Lond. B Biol. Sci. **264:**1457–1461.
17. **Flano, E., S. M. Husain, J. T. Sample, D. L. Woodland, and M. A. Blackman.** 2000. Latent murine gamma-herpesvirus infection is established in activated B cells, dendritic cells, and macrophages. J. Immunol. **165:**1074–1081.
18. **Flano, E., Q. Jia, J. Moore, D. L. Woodland, R. Sun, and M. A. Blackman.** 2005. Early establishment of gamma-herpesvirus latency: implications for immune control. J. Immunol. **174:**4972–4978.
19. **Flano, E., I. J. Kim, D. L. Woodland, and M. A. Blackman.** 2002. Gamma-herpesvirus latency is preferentially maintained in splenic germinal center and memory B cells. J. Exp. Med. **196:**1363–1372.
20. **Flynn, J. L., and J. Chan.** 2005. What's good for the host is good for the bug. Trends Microbiol. **13:**98–102.
21. **Husain, S. M., E. J. Usherwood, H. Dyson, C. Coleclough, M. A. Coppola, D. L. Woodland, M. A. Blackman, J. P. Stewart, and J. T. Sample.** 1999. Murine gammaherpesvirus M2 gene is latency-associated and its protein a target for CD8(+) T lymphocytes. Proc. Natl. Acad. Sci. U. S. A. **96:**7508–7513.
22. **Kim, I. J., E. Flano, D. L. Woodland, F. E. Lund, T. D. Randall, and M. A. Blackman.** 2003. Maintenance of long term gamma-herpesvirus B cell latency is dependent on CD40-mediated development of memory B cells. J. Immunol. **171:**886–892.
23. **Kipar, A., K. Kohler, W. Leukert, and M. Reinacher.** 2001. A comparison of lymphatic tissues from cats with spontaneous feline infectious peritonitis (FIP), cats with FIP virus infection but no FIP, and cats with no infection. J. Comp. Pathol. **125:**182–191.
24. **Kipar, A., H. May, S. Menger, M. Weber, W. Leukert, and M. Reinacher.** 2005. Morphologic features and development of granulomatous vasculitis in feline infectious peritonitis. Vet. Pathol. **42:**321–330.
25. **Macrae, A. I., B. M. Dutia, S. Milligan, D. G. Brownstein, D. J. Allen, J. Mistrikova, A. J. Davison, A. A. Nash, and J. P. Stewart.** 2001. Analysis of a novel strain of murine gammaherpesvirus reveals a genomic locus important for acute pathogenesis. J. Virol. **75:**5315–5327.
26. **Martin, A. P., C. Canasto-Chibuque, L. Shang, B. J. Rollins, and S. A. Lira.** 2006. The chemokine decoy receptor M3 blocks CC chemokine ligand 2 and CXC chemokine ligand 13 function in vivo. J. Immunol. **177:**7296–7302.
27. **Moyron-Quiroz, J. E., J. Rangel-Moreno, K. Kusser, L. Hartson, F. Sprague, S. Goodrich, D. L. Woodland, F. E. Lund, and T. D. Randall.** 2004. Role of inducible bronchus associated lymphoid tissue (iBALT) in respiratory immunity. Nat. Med. **10:**927–934.
28. **Nash, A. A., B. M. Dutia, J. P. Stewart, and A. J. Davison.** 2001. Natural history of murine gamma-herpesvirus infection. Phil. Trans. R. Soc. Lond. B Biol. Sci. **356:**569–579.
29. **O'Connor, C. M., and D. H. Kedes.** 2007. Rhesus monkey rhadinovirus: a model for the study of KSHV. Curr. Top. Microbiol. Immunol. **312:**43–69.
30. **Parry, C. M., J. P. Simas, V. P. Smith, C. A. Stewart, A. C. Minson, S. Efstathiou, and A. Alcami.** 2000. A broad spectrum secreted chemokine binding protein encoded by a herpesvirus. J. Exp. Med. **191:**573–578.
31. **Renne, R., D. Dittmer, D. Kedes, K. Schmidt, R. C. Desrosiers, P. A. Luciw, and D. Ganem.** 2004. Experimental transmission of Kaposi's sarcoma-associated herpesvirus (KSHV/HHV-8) to SIV-positive and SIV-negative rhesus macaques. J. Med. Primatol. **33:**1–9.
32. **Rivailler, P., A. Carville, A. Kaur, P. Rao, C. Quink, J. L. Kutok, S. Westmoreland, S. Klumpp, M. Simon, J. C. Aster, and F. Wang.** 2004. Experimental rhesus lymphocryptovirus infection in immunosuppressed macaques: an animal model for Epstein-Barr virus pathogenesis in the immunosuppressed host. Blood **104:**1482–1489.
33. **Sangster, M. Y., D. J. Topham, S. D'Costa, R. D. Cardin, T. N. Marion, L. K. Myers, and P. C. Doherty.** 2000. Analysis of the virus-specific and nonspecific B cell response to a persistent B-lymphotropic gammaherpesvirus. J. Immunol. **164:**1820–1828.
34. **Scalzo, A. A., A. J. Corbett, W. D. Rawlinson, G. M. Scott, and M. A. Degli-Esposti.** 2007. The interplay between host and viral factors in shaping the outcome of cytomegalovirus infection. Immunol. Cell Biol. **85:**46–54.
35. **Staeheli, P., R. Grob, E. Meier, J. G. Sutcliffe, and O. Haller.** 1988. Influenza virus-susceptible mice carry Mx genes with a large deletion or a nonsense mutation. Mol. Cell. Biol. **8:**4518–4523.
36. **Stevenson, P. G., and P. C. Doherty.** 1998. Kinetic analysis of the specific host response to a murine gammaherpesvirus. J. Virol. **72:**943–949.
37. **Stewart, J. P., N. Micali, E. J. Usherwood, L. Bonina, and A. A. Nash.** 1999. Murine gamma-herpesvirus 68 glycoprotein 150 protects against virus-induced mononucleosis: a model system for gamma-herpesvirus vaccination. Vaccine **17:**152–157.

38. **Stewart, J. P., E. J. Usherwood, A. Ross, H. Dyson, and T. Nash.** 1998. Lung epithelial cells are a major site of murine gammaherpesvirus persistence. J. Exp. Med. **187:**1941–1951.
39. **Sunil-Chandra, N. P.** 1991. Studies on the pathogenesis of a murine gammaherpesvirus (MHV-68). Ph.D. thesis. University of Cambridge, Cambridge, United Kingdom.
40. **Sunil-Chandra, N. P., S. Efstathiou, J. Arno, and A. A. Nash.** 1992. Virological and pathological features of mice infected with murine gamma-herpesvirus 68. J. Gen. Virol. **73:**2347–2356.
40a. **Szakal, A. K., J. K. Taylor, J. P. Smith, M. H. Kosco, G. F. Burton, and J. J. Tew.** 1990. Kinetics of germinal center development in lymph nodes of young and aging immune mice. Anat. Rec. **227:**475–185.
41. **Terry, L. A., J. P. Stewart, A. A. Nash, and J. K. Fazakerley.** 2000. Murine gammaherpesvirus-68 infection and persistence in the central nervous system. J. Gen. Virol. **81:**2635–2643.
42. **Usherwood, E. J., A. J. Ross, D. J. Allen, and A. A. Nash.** 1996. Murine gammaherpesvirus-induced splenomegaly: a critical role for CD4 T cells. J. Gen. Virol. **77:**627–630.
43. **Usherwood, E. J., J. P. Stewart, K. Robertson, D. J. Allen, and A. A. Nash.** 1996. Absence of splenic latency in murine gammaherpesvirus 68-infected B cell-deficient mice. J. Gen. Virol. **77:**2819–2825.
44. **van Berkel, V., J. Barrett, H. L. Tiffany, D. H. Fremont, P. M. Murphy, G. McFadden, S. H. Speck, and H. W. Virgin.** 2000. Identification of a gammaherpesvirus selective chemokine binding protein that inhibits chemokine action. J. Virol. **74:**6741–6747.
45. **van Berkel, V., B. Levine, S. B. Kapadia, J. E. Goldman, S. H. Speck, and H. W. T. Virgin.** 2002. Critical role for a high-affinity chemokine-binding protein in gamma-herpesvirus-induced lethal meningitis. J. Clin. Investig. **109:**905–914.
46. **Weck, K. E., S. S. Kim, H. W. Virgin, and S. H. Speck.** 1999. Macrophages are the major reservoir of latent murine gammaherpesvirus 68 in peritoneal cells. J. Virol. **73:**3273–3283.
47. **Wheat, W. H., C. D. Cool, Y. Morimoto, P. R. Rai, C. H. Kirkpatrick, B. A. Lindenbaum, C. A. Bates, M. C. Ellison, A. E. Serls, K. K. Brown, and J. M. Routes.** 2005. Possible role of human herpesvirus 8 in the lymphoproliferative disorders in common variable immunodeficiency. J. Exp. Med. **202:**479–484.
48. **Willer, D. O., and S. H. Speck.** 2003. Long-term latent murine gammaherpesvirus 68 infection is preferentially found within the surface immunoglobulin D-negative subset of splenic B cells in vivo. J. Virol. **77:**8310–8321.